

Hydrodynamics of compression of a plasma with a frozen-in magnetic field by a thin cylindrical wall

V. L. Velikovich, S. M. Gol'berg, M. A. Liberman, and F. S. Felber¹⁾

Institute of Physics Problems, USSR Academy of Sciences

(Submitted 12 June 1984)

Zh. Eksp. Teor. Fiz. **88**, 445–460 (February 1985)

The hydrodynamics of a dense plasma containing a magnetic field and compressed by a thin cylindrical wall is considered. Self-similar solutions are obtained for the compression of the plasma by the wall, and the structure of the plasma boundary layer near the compressing wall is obtained. It is shown that formation of a boundary layer and the produced thermal and thermomagnetic fluxes increase substantially the diamagnetism of the plasma. The magnetic-flux loss upon compression of a plasma with classical transport coefficients can increase substantially, right up to the corresponding values for a turbulent plasma. It is shown that at moderate and experimentally attainable rates of plasma compression by a cylinder wall magnetic-flux losses are low and effective compression of a magnetic-field frozen in the plasma by a cylinder wall is feasible. Numerical calculations of radial compression of a plasma with a magnetic field by a cylinder agree well with the self-similar solutions obtained. Numerical simulation of the problem shows that in the procedure considered the compression of the magnetic field depends little on the equation of state of the cylinder walls and on the cylinder heat capacity, conductivity, and compressibility.

INTRODUCTION

The possibility of using new methods to obtain in the laboratory ultrastrong magnetic fields on the order of 100 MOe and more were estimated in Refs. 1–4. The first indications of the possibility of compressing strongly a magnetic field via laser ablation are contained in Refs. 5 and 6.²⁾ Estimates are presented for two possible methods of rapidly compressing a plasma with a frozen-in magnetic field, by using a thin cylindrical wall, and in a Z pinch with a trapped external magnetic field. It is known, however, that the flows and inhomogeneities that are produced when a plasma is heated lead to an anomalously rapid diffusion of the magnetic field. We consider here the dynamics of compression of a plasma with a frozen-in magnetic field by assuming for the plasma classical transport coefficients. We show that although the diamagnetic flows produced in the plasma decrease effectively the magnetic Reynolds number, they nevertheless do not hinder the compression of the magnetic field in accordance with the estimates of Refs. 1–4. Similar calculations with the transport coefficients for a turbulent plasma do not lead to a more substantial diamagnetism.

We consider the hydrodynamics of compression of a plasma with a magnetic field by a thin cylindrical wall whose initial kinetic energy was acquired by the action of several-kilobar pressure produced by cylindrically-symmetric irradiation of outer wall surface by a laser pulse or by an electron or ion beam. For example, examples on acceleration of foils by a laser⁷ show that the observed velocities for foils several micron thick can reach $(1-2) \cdot 10^7$ cm/s. We note that in contrast to the traditional methods of generating strong pulsed magnetic-fields by implosive compression,⁸ in this case the thin walls of the cylinder are by themselves inessential for the magnetic-field compression proper. The magnetic flux

diffuses freely through the thin walls of the shell, and the shell kinetic energy E_0 goes to compression of the plasma with the frozen-in magnetic field. The simplest necessary condition that the magnetic field be frozen in the plasma is formulated as a constraint on the magnetic Reynolds number: $Rm_0 = 4\pi\sigma uR/c^2$, where σ , u , and R are respectively the characteristic values of the conductivity, velocity, and boundary radius of the plasma cylinder. When this constraint is satisfied, it can be easily seen that if $\beta_0 = 16\pi n_0 T_0 / H_0^2 \ll 1$, the magnetic field is compressed from an initial value H_0 (at $R = R_0$) to a final value $H_f = H_0/\delta$, where $\delta = H_0^2 R_0^2 L / 8E_0$ is the ratio of the magnetic energy inside the shell to the kinetic energy of the shell (L is the length of the shell). In subsonic compression of the plasma by the shell, the only compression that we shall consider, the total pressure inside the plasma cylinder remains approximately uniform over the cross section during the entire compression process. An important role in the compression of the magnetic flux in a plasma can therefore be played by redistribution of the initial uniform density over the radius, i.e., by formation, next to the wall, of a boundary layer in which $\beta \gtrsim 1$. The magnetic-flux losses on compression are therefore determined not by the value of Rm_0 , but by some effective Reynolds number value that takes into account the profiles of the density, temperature, magnetic field, and velocity that are produced in the plasma. Since these profiles have large gradients at the cylinder wall, a substantial role can be played, generally speaking, by the thermal conductivity of the plasma and by the thermomagnetic effects. Similar anomalies of the magnetic-flux losses arise, e.g., in plasma configuration with reversed magnetic field.⁹

In the first part of this paper we consider the self-similar solutions of the equations of one-fluid hydrodynamic plasma, which describe cylindrically symmetric compression of

a plasma with a magnetic field. The self-similar solution obtained permit an estimate of the roles of the different processes in the formation of the boundary layer at the wall and to calculate the losses of the magnetic flux when plasma is compressed.

In the second part of the paper we present the results of a numerical integration of the complete one-dimensional hydrodynamic-equation system that describes the compression of the plasma by the shell. The result of the numerical simulation of the plasma compression, with allowance for the energy lost to radiation, agree well with the self-similar solutions described in the first part. In particular, the numerical calculations demonstrate the high efficiency with which the plasma with the magnetic field are compressed by the shell, and the weak dependence of the results on the equation of state of the shell and on its conductivity, thermal conductivity, heat capacity, and compressibility. The end-face losses due to plasma spreading in the axial dimension are likewise insignificant as a rule.

2. INITIAL EQUATIONS

Consider cylindrically symmetric compression of a plasma with a frozen-in magnetic field directed along the cylinder axis, taken to be the z axis. We assume the problem to be one-dimensional, so that all the quantities are homogeneous in z , and their gradients are directed along the radius. Slow (subsonic) flow of a dense plasma is described by the single-temperature ($T_e = T_i = T$) single-fluid hydrodynamic equations of the plasma, for the transport coefficients of which we assume the known classical values.¹⁰ We write down these equations, neglecting small viscous terms:

$$\partial n / \partial t + \operatorname{div} (nu) = 0, \quad (2.1)$$

$$\frac{\partial \mathbf{H}}{\partial t} = \operatorname{rot} \left\{ [\mathbf{u} \times \mathbf{H}] - \frac{c\mathbf{R}}{en} \right\}, \quad (2.2)$$

$$\rho \left[\frac{\partial \mathbf{u}}{\partial t} + (\mathbf{u} \nabla) \mathbf{u} \right] = \frac{1}{c} [\mathbf{j} \times \mathbf{H}] - \nabla P, \quad (2.3)$$

$$\mathbf{j} = \frac{c}{4\pi} \operatorname{rot} \mathbf{H}, \quad (2.4)$$

$$\begin{aligned} & \frac{3}{2} n \left[\frac{\partial T}{\partial t} + (\mathbf{u} \nabla) T \right] + P \operatorname{div} u \\ & = -\operatorname{div} (\mathbf{q}_e + \mathbf{q}_i) + \frac{j^2}{\sigma} + \frac{\mathbf{j} \mathbf{R}_T}{en} - Q_r. \end{aligned} \quad (2.5)$$

Here n is the electron and ion density in the quasineutral plasma ($n_e = n_i \equiv n$); $\rho = m_i n$ is the mass density; \mathbf{j} is the electric-current density; \mathbf{u} is the plasma-flow velocity transverse to the magnetic field (in our formulation of the plasma only the radial plasma velocity differs from zero); $P = 2nT$ is the kinetic pressure of the plasma, σ is the plasma conductivity; q_0 and q_1 are the electron and ion heat fluxes, respectively; \mathbf{R} is the total friction force due to momentum transfer in electron and ion collisions; \mathbf{R}_T is the friction-force component due to the temperature gradient (thermoforce); Q_r are the volume energy losses corresponding to radiation of the plasma. The expressions for the fluxes and for the corresponding kinetic coefficients are well known,¹⁰ but are too long to present here.

Equations (2.1)–(2.5) constitute the complete system of equations that describes the plasma compression hydrodynamics. In the case of an infinitely thin nonconducting shell, the boundary condition on the shell surface is $r = R(t)$ for the magnetic field

$$\mathbf{H}(r=R(t)) = \mathbf{H}_{\text{ext}}(t), \quad (2.6)$$

where $\mathbf{H}_{\text{ext}}(t)$ is the external magnetic field. The second boundary condition for \mathbf{H} follows naturally from the fact that \mathbf{H} is regular at $r = 0$:

$$(\partial \mathbf{H} / \partial r)_{r=0} = 0. \quad (2.7)$$

The boundary condition for the radial component of the velocity $u \equiv u_r$ is

$$u(r=R(t)) = \dot{R}(t), \quad u(r=0) = 0. \quad (2.8)$$

The boundary conditions for the temperature depend on the equations of state of the shell material. Two extreme cases are zero heat conductivity at the boundary, i.e., a zero plasma-temperature gradient at the plasma-shell boundary, and a constant temperature, meaning infinite heat capacity, of the shell. In addition, a natural condition is that the functions n and T be regular at $r = 0$.

We introduce the magnetic viscosity $\nu_m = c^2 / 4\pi\sigma$ and determine the dimensionless parameter that characterizes the freezing-in of the magnetic field into the plasma when the latter is compressed—the magnetic Reynolds number

$$\operatorname{Rm} = \nu L / \nu_m, \quad (2.9)$$

the ν , L , and ν_m are the characteristic values of the velocity, of the transverse dimension, and of the magnetic viscosity, respectively. The highest value $\operatorname{Rm} = \operatorname{Rm}_0$ corresponds to the largest value of the velocity $v = |\dot{R}(t)|$ and of the radius $L = R(t)$, and the lowest value of the magnetic viscosity. For the sake of argument we put also $\nu_m = \nu_m(r = R(t))$, which corresponds in general to a thermally insulating shell with low heat capacity. We define thus

$$\operatorname{Rm}_0 = R(t) |\dot{R}(t)| / \nu_m(R(t)). \quad (2.10)$$

We introduce also the effective magnetic Reynolds number defined as the ratio of the characteristic variation times of the magnetic flux Φ and of the plasma compression:

$$\operatorname{Rm}_{\text{eff}} = \frac{\Phi(t) / |\dot{\Phi}(t)|}{R(t) / |\dot{R}(t)|}. \quad (2.11)$$

The quantity (2.11) characterizes the magnetic-flux losses. Assuming $\operatorname{Rm}_{\text{eff}}(t) = \text{const}$ (or, equivalently, choosing appropriately the time-averaged value of $\operatorname{Rm}_{\text{eff}}$), we obtain

$$\Phi / \Phi_0 = (R / R_0)^{1 / \operatorname{Rm}_{\text{eff}}}. \quad (2.12)$$

Accordingly, we have for the compression of the magnetic field the estimate

$$H / H_0 \approx (R_0 / R)^{2 - 4 / \operatorname{Rm}_{\text{eff}}}. \quad (2.13)$$

In particular, if the thermoforce in (2.2) can be neglected, expression (2.11) is equivalent to

$$\operatorname{Rm}_{\text{eff}} = |\dot{R}(t)| \int_0^{R(t)} H r dr / \nu_m(R(t)) R^2(t) (\partial H / \partial r)_{r=R(t)}. \quad (2.14)$$

The simplest estimate in accord with Eq. (2.14) [the integral of the numerator is estimated at $HR^2(t)$ and the derivative in the denominator at $H/R(t)$] leads to expression (2.10) for Rm_0 . In the general case, however, Rm_{eff} , and hence also the magnetic-field compression, depends substantially on the temperature and magnetic-field profiles produced in the course of the compression, and can be determined only by solving the hydrodynamic problem.

We consider the solutions of Eq. (2.1)–(2.5) for two limiting cases corresponding to compression of a nonmagnetized plasma $\Omega_e \tau_e \ll 1$ and a fully magnetized plasma ($1 \ll \Omega_i \tau_i \ll \Omega_e \tau_e$; here $\Omega_{e,i}$ and $\tau_{e,i}$ are respectively the cyclotron frequencies and the collision times for the electrons and ions). In Secs. 3 and 4 below we do not take into account the energy lost to radiation and neglect the heat capacity of the shell.

3. SELF-SIMILAR SOLUTIONS FOR A NONMAGNETIZED PLASMA

In the case of a nonmagnetized plasma, the contribution of the thermoforce to the friction force is negligible, i.e., we can substitute in (2.2)

$$\mathbf{R} = \mathbf{R}_u + \mathbf{R}_r \approx \mathbf{R}_u = en\mathbf{j}/\sigma. \quad (3.1)$$

Those terms in the right-hand side of (2.5), which represent the heat fluxes and the heat-release associated with the thermoforce, are also small compared with the Joule heating. As a result, eliminating the current density with the aid of (2.4) and transforming to a cylindrical coordinate frame, we obtain the following system of equations:

$$\frac{\partial n}{\partial t} + \frac{1}{r} \frac{\partial}{\partial r} (rnu) = 0, \quad (3.2)$$

$$\frac{\partial H}{\partial t} + \frac{1}{r} \frac{\partial}{\partial r} (rHu) = \frac{1}{r} \frac{\partial}{\partial r} \left(r v_m \frac{\partial H}{\partial r} \right), \quad (3.3)$$

$$3n \left(\frac{\partial T}{\partial t} + u \frac{\partial T}{\partial r} \right) + \frac{2nT}{r} \frac{\partial}{\partial r} (ru) = \frac{v_m}{4\pi} \left(\frac{\partial H}{\partial r} \right)^2, \quad (3.4)$$

$$\frac{\partial}{\partial r} \left(2nT + \frac{H^2}{8\pi} \right) = 0. \quad (3.5)$$

Equation (3.5) follows from (2.3) and means that the total pressure in subsonic flow is uniform.

We introduce in Eqs. (3.2)–(3.5) a new independent variable

$$\xi = r/R(t), \quad (3.6)$$

where $R(t)$ corresponds to the boundary of the compressed plasma cylinder. We seek the self-similar solutions of the system (3.2)–(3.5), for which all the variables are functions of ξ and t of the form

$$u(r, t) = \dot{R}(t) U(\xi), \quad n(r, t) = n_0 \frac{R_0^2}{R^2(t)} N(\xi), \quad (3.7)$$

$$H(r, t) = H_0 h(\xi) B(\xi), \quad T(r, t) = T_0 \theta(\xi) \Theta(\xi).$$

Here $R_0 = R(t=0)$ is the initial radius of the plasma cylinder, while n_0 , H_0 , and T_0 are as-yet arbitrary constants with dimensions of the particle-number density, magnetic field, and temperature, respectively.

The time dependence of the magnetic field in (3.7) is

compatible with the boundary condition (2.6) at a constant field outside the cylinder only if $H_{ext} = 0$. We have then from (2.6), (2.7), and (2.8)

$$B(\xi=1) = 0, \quad (dB/d\xi)_{\xi=0} = 0, \quad (3.8)$$

$$U(\xi=1) = 1. \quad (3.9)$$

The initial conditions are

$$a(t=0) = h(t=0) = \theta(t=0) = 1, \quad (3.10)$$

where $a(t) = R(t)/R_0$.

Transforming in (3.5) to the variable (3.7) we find, taking (3.10) into account

$$\theta(t) = a^2(t) h^2(t), \quad (3.11)$$

$$(16\pi n_0 T_0 / H_0^2) N\Theta + B^2 = \text{const.} \quad (3.12)$$

$$a^2(t) h^2(t) (16\pi^{-1} n_0^{-2} T_0^2 / H_0^2) N\Theta + \theta(t)^2 B^2$$

$$= (dB^2/d^2\xi^2)_{\xi=0} = \text{const.}$$

For $N(\xi)$ and $\Theta(\xi)$ we assume the boundary conditions

$$N(\xi=1) = \Theta(\xi=1) = 1 \quad (3.13)$$

and eliminate the leeway in the choice of the normalization constant, putting

$$16\pi n_0 T_0 / H_0^2 = 1. \quad (3.14)$$

When account is taken of (3.8) and (3.13), Eq. (3.12) takes then a particularly simple form

$$N\Theta + B^2 = 1. \quad (3.15)$$

From (3.2), taking (3.9) into account, we have

$$U(\xi) = \xi. \quad (3.16)$$

Substituting (3.7) in (3.3) and using (3.16), we obtain after separating the variables ξ and t

$$\frac{1}{\xi} \frac{d}{d\xi} \left(\xi \Theta^{-1/2} \frac{dB}{d\xi} \right) + \mu^2 B = 0, \quad (3.17)$$

$$\frac{\dot{h}}{h} + 2 \frac{\dot{a}}{a} = -\mu^2 \frac{v_m^{(0)}}{a^2 \theta^{1/2}}, \quad (3.18)$$

where $\lambda_2 = \text{const}$ is the separation constant, and $v_m^{(0)} = v_m(t=0, r=R_0)/R_0^2$.

Substituting (3.7) in (3.4) and using (3.15) and (3.16), we obtain after separating the variables

$$\Theta^{-1/2} (dB/d\xi)^2 = \lambda^2 (1 - B^2), \quad (3.19)$$

$$\frac{\dot{a}}{a} + \frac{3}{4} \frac{\dot{\theta}}{\theta} = \lambda^2 \frac{v_m^{(0)}}{a^2 \theta^{1/2}}, \quad (3.20)$$

where λ^2 is the separation constant.

Putting

$$\xi = \lambda^2 / \mu^2, \quad (3.21)$$

we get from (3.11), (3.18), and (3.20)

$$a(t) = (1 + 2\lambda^2 v_m^{(0)} t)^{-(2\xi+3)/2\xi}, \quad (3.22)$$

$$h(t) = (1 + 2\lambda^2 v_m^{(0)} t)^{(4\xi+5)/2\xi}, \quad (3.23)$$

$$\theta(t) = (1 + 2\lambda^2 v_m^{(0)} t)^{(2\xi+2)/\xi}. \quad (3.24)$$

We obtain thus a one-parameter family of solutions that

depend on the parameter ζ . The values of Rm_0 and Rm_{eff} , which are defined in (2.10) and (2.11), are in this case

$$Rm_0 = \mu^2(2\zeta + 3), \quad (3.25)$$

$$Rm_{eff} = 2\zeta + 3. \quad (3.26)$$

It can be seen that for each self-similar solution the magnetic Reynolds numbers, both Rm_0 and Rm_{eff} , are constants independent of time. Consequently $\lambda^2 > 0$ and $\zeta > -3/2$ for solutions described by $Rm_0 > 0$ and $Rm_{eff} > 0$, respectively.

At $\zeta > 0$ the self-similar solutions correspond to infinite compression of the magnetic field, as $t \rightarrow \infty$, in accordance with the power law that follows from (3.22). The slowest compression pertains to the highest Rm values corresponding to $\zeta \rightarrow \infty$, in which case $a(t) \propto 1/t$ (we note that as $H \rightarrow \infty$ we have $\Phi \rightarrow 0$). The value $\zeta = 0$ corresponds to compression in accordance with a power law

$$a(t) = \exp(-3\mu_0^2 \nu_m^{(0)} t), \quad (3.27)$$

$$h(t) = \exp(5\mu_0^2 \nu_m^{(0)} t), \quad (3.28)$$

$$\theta(t) = \exp(4\mu_0^2 \nu_m^{(0)} t), \quad (3.29)$$

where $\lambda_0^2 = \lambda^2(\zeta = 0)$. Negative values of ζ correspond to solutions with small $Rm_{eff} < 3$, which describe compression of the magnetic field to infinity within finite time intervals.

The permissible range of ζ is determined by the condition for the existence of the self-similar profiles $B(\xi)$, $\Theta(\xi)$, and $N(\xi)$, which satisfy the boundary conditions. Eliminating Θ from (3.17) and (3.19), we obtain

$$\frac{d^2 B}{d\xi^2} - \frac{1}{\xi} \frac{dB}{d\xi} + \frac{(2-\zeta^{-1})B}{1-B^2} \left(\frac{dB}{d\xi} \right)^2 = 0. \quad (3.30)$$

The solution (3.30) with boundary condition (3.8) solves the problem completely: $\Theta(\xi)$ and $N(\xi)$ are expressed then with the aid of (3.19) and (3.15), and for λ we have

$$\lambda^2 = (dB/d\xi)_{\xi=1}^2. \quad (3.31)$$

Nontrivial solutions of Eq. (3.30) exist at $B(0) = 1$. The point $\xi = 0$ is then a singular point of Eq. (3.30). Near this point we have

$$1-B(\xi) \propto \xi^{4\zeta}, \quad \Theta(\xi) \propto \xi^{4(2\zeta-1)/3}, \quad N(\xi) \propto \xi^{4(\zeta+1)/3}. \quad (3.32)$$

From the condition that $\Theta(\xi)$ be regular at $\xi = 0$, it follows that

$$\zeta \geq 1/2. \quad (3.33)$$

Transforming in (3.30) to a new independent variable $\eta = \xi^2$ we obtain immediately its solution with the boundary condition (3.31)

$$\xi = \left[\frac{2}{\lambda} \int_B^1 (1-z^2)^{1/2\zeta-1} dz \right]^{1/2}. \quad (3.34)$$

When (33) is satisfied, the second boundary condition of (3.8) is satisfied automatically, while the first condition [$B(1) = 0$] makes it possible to determine the value $\lambda(\zeta)$:

$$\lambda(\zeta) = \Gamma(1/2\zeta) \Gamma(1/2) \Gamma(1/2\zeta + 1/2). \quad (3.35)$$

In particular, for the minimum value $\zeta = 1/2$ the solution (3.34) takes the rather simple form

$$B(\xi) = 1 - \xi^2. \quad (3.36)$$

In this case $\lambda^2 = 4$, $\lambda = 2$, and the corresponding minimum values of the magnetic Reynolds numbers, at which compression of the magnetic field is possible, are $Rm_0 = 32$ and $Rm_{eff} = 4$. It can be seen from (3.34) and (3.35) that self-similar solutions that satisfy the boundary conditions (3.8) exist in the entire range (3.33). The magnetic Reynolds numbers Rm_0 and Rm_{eff} increase with increasing ζ [see (3.25), (3.26), and (3.35)], i.e., their ranges are

$$32 \leq Rm_0 < \infty, \quad 4 \leq Rm_{eff} < \infty. \quad (3.37)$$

At $\zeta \gg 1$ we obtain from (3.35) the estimate

$$\lambda = 2\zeta + 2 \ln 2 + O(1/\zeta), \quad (3.38)$$

which establishes the asymptotic connection between Rm_0 and Rm_{eff} for large magnetic Reynolds numbers:

$$Rm_{eff} \approx (Rm_0/2)^{1/2}. \quad (3.39)$$

An exact calculation by Eq. (3.35) shows that the asymptotic equation is indeed a good approximation in the entire range of ζ (see Fig. 4 below).

With the aid of the solution (3.34), which determines the profiles of $B(\xi)$, it is easy to obtain expressions for $\Theta(\xi)$ and $N(\xi)$:

$$\Theta(\xi) = \xi^{4\zeta} [1 - B^2(\xi)]^{7\zeta(1-\zeta)}, \quad (3.40)$$

$$N(\xi) = \xi^{-4\zeta} [1 - B^2(\xi)]^{1/2(1+2\zeta)}. \quad (3.41)$$

As can be seen from Eqs. (3.34), (3.40), and (3.41), the quantities $B(\xi)$, $N(\xi)$ and $\Theta(\xi)$ are practically uniform over the entire plasma volume, except for the wall boundary layer the wall of width $1/\zeta$ at $\zeta \gg 1$. In this layer $B(\xi)$, $N(\xi)$, and $\Theta(\xi)$ vary from the values on the axis to the boundary values, and it is this which causes the appreciable difference between Rm_{eff} and Rm_0 . Thus, formation of a boundary layer near the wall that compresses the plasma indeed increases the magnetic-flux losses, owing to the large gradient of the magnetic field in the boundary layer, and this manifests itself in the substantially slower growth of Rm_{eff} compared with Rm_0 .

Obviously, at all values of the magnetic Reynolds number in the range (3.37) the condition $\Omega_e \tau_e \ll 1$, which is valid at $t = 0$, ceases to hold starting with some instant of time, in accordance with (3.22)–(3.24). The solution obtained above is then no longer valid, for in the case of a magnetized plasma the kinetic coefficients are changed, and the terms of (2.1)–(2.5) that could be neglected in Eqs. (2.1)–(2.5) at $\Omega_e \tau_e \ll 1$ now become significant. The solutions described here can in this case be regarded only as model-dependent and take only qualitatively into account the influence of the finite plasma conductivity on the hydrodynamics of the compression.

4. SELF-SIMILAR SOLUTIONS FOR A MAGNETIZED PLASMA

We find now the self-similar solutions of Eqs. (2.1–2.5), satisfying the same boundary conditions as the solutions considered in Sec. 3, for the opposite limiting case of a fully magnetized plasma, when $\Omega_e \tau_e \gg \Omega_i \tau_i \gg 1$. It must be noted

here that the first of the boundary conditions (3.8) is obviously formally incompatible with the condition that the plasma is fully magnetized. If, however, the temperature and the magnetic field are high enough, the point at which $\Omega_i \tau_i = 1$ is arbitrarily close to the boundary $r = R_0$ at the initial instant, and comes closer to it in the course of the compression. Thus, solutions corresponding to the considered limiting case, together with the solutions investigated in the preceding section, determine the upper and lower bounds of the range of Rm_{eff} , as is indeed confirmed by numerical calculations (see Sec. 5 below).

We rewrite Eqs. (2.1)–(2.5) for a magnetized plasma, using the corresponding expression of Ref. 10 for the kinetic coefficient, the friction force, and the heat fluxes. Obviously, Eqs. (2.1) and (2.4) remain unchanged. The terms that describe the thermal conductivity of the plasma (determined in this case by the ion rather than by the electron conductivity), the heat flux due to the relative motion of the electrons and ions, and the thermoforce turn out to be here of the same order as the Joule friction as the heating. As a result, Eqs. (2.2) and (2.5), written in cylindrical coordinates, take apart from terms small in the parameters $1/(\Omega_i \tau_i)$ and $(m_e/m_i)^{1/2}$, the form

$$\frac{\partial H}{\partial t} + \frac{1}{r} \frac{\partial}{\partial r} (rHu) = \frac{1}{r} \frac{\partial}{\partial r} r v_m \left(\frac{\partial H}{\partial r} + \frac{6\pi n}{H} \frac{\partial T}{\partial r} \right), \quad (4.1)$$

$$\begin{aligned} 3n \left(\frac{\partial T}{\partial t} + u \frac{\partial T}{\partial r} \right) + \frac{2nT}{r} \frac{\partial}{\partial r} (ru) \\ = \frac{v_m}{4\pi} \frac{\partial H}{\partial r} \left[\frac{\partial H}{\partial r} + \frac{6\pi n}{H} \frac{\partial T}{\partial r} \right] \\ + \frac{3}{2r} \frac{\partial}{\partial r} \left(r v_m \frac{nT}{H} \frac{\partial H}{\partial r} \right) \\ + \frac{1}{4} \left(\frac{2m_i}{m_e} \right)^{1/2} \frac{1}{r} \frac{\partial}{\partial r} \left(\frac{16\pi n T}{H^2} r v_m n \frac{\partial T}{\partial r} \right). \end{aligned} \quad (4.2)$$

Equations (4.1) and (4.2) are solved simultaneously with Eqs. (3.2) and (3.5), which, of course retain the same form. Transforming in these equations to the self-similar variables (3.6) and (3.7), we obtain equations that are similar in many respects to those given in Sec. 3. In particular, the velocity profile has the form (3.16) as before, the time dependences of the functions $a(t)$, $h(t)$, and $\theta(t)$ are given by Eqs. (3.22)–(3.24), while expressions (3.25) and (3.26) remain valid for the Reynolds numbers. In this case, however, the permissible range of ζ and the values of constants λ^2 and λ^2 , determined for a given value of ζ from the conditions that there exist profiles $B(\xi)$, $\Theta(\xi)$ and $N(\xi)$ that satisfy the boundary conditions, must be obtained with the aid of the following equations:

$$\frac{1}{\xi} \frac{d}{d\xi} \xi \left[Y \frac{dB}{d\xi} - \frac{1-B^2}{4B} \frac{dY}{d\xi} \right] + \mu^2 B = 0, \quad (4.3)$$

$$\begin{aligned} \left(\frac{dB}{d\xi} \right) \left[Y \frac{dB}{d\xi} - \frac{1-B^2}{4B} \frac{dY}{d\xi} \right] \\ + \frac{1}{\xi} \frac{d}{d\xi} \left\{ \frac{3}{8} \frac{(1-B^2)}{B^2} \left[Y \frac{dB}{d\xi} - A \frac{1-B^2}{4B} \frac{dY}{d\xi} \right] \right\} \\ = \lambda^2 (1-B^2). \end{aligned} \quad (4.4)$$

We have introduced here the notation

$$Y(\xi) = \Theta(\xi)^{-1/2}, \quad A = \frac{4}{9} \left(\frac{2m_i}{m_e} \right)^{1/2}. \quad (4.5)$$

Equations (4.3) and (4.4) are solved with the same boundary conditions (3.8) and (3.13) (and under the same supplementary assumption $B(0) = 1$) as Eqs. (3.17) and (3.19). The points $\xi = 0$ and $\xi = 1$ are singular points of this system of equations. It is easy to show that near $\xi = 0$ we have

$$1-B(\xi) \propto \xi^s, \quad Y(\xi) \propto \xi^{2-s}, \quad (4.6)$$

where $s = (6A + 16\zeta)/(3A - 2)$.

From the condition that $\Theta(\xi)$ be regular at $\xi = 0$ it follows that $s \geq 2$, and we thus obtain

$$\xi \geq -1/4. \quad (4.7)$$

It can be shown that the solutions of Eqs. (4.3) and (4.4), which satisfy the necessary boundary conditions exist for all ζ under condition (4.7). Figure 1 shows the profiles of $B(\xi)$, $\Theta(\xi)$, and $N(\xi)$ for a number of values ζ . The value of Rm_{eff} at (4.7) is 2.5, and the numerically determined corresponding value of Rm_0 is 14.2. This means that for the considered family of solutions we have

$$14.2 \leq Rm_0 < \infty, \quad 2.5 \leq Rm_{\text{eff}} < \infty. \quad (4.8)$$

At the singular point $\xi = 1$ we have $B = 0$ and $dY/d\xi = 0$. It can be shown that the heat flux at the boundary (at $\xi = 1$), which is proportional to the expression in the curly brackets in the last term of the left hand side of (4.4), is finite and positive. This circumstance can be interpreted as the

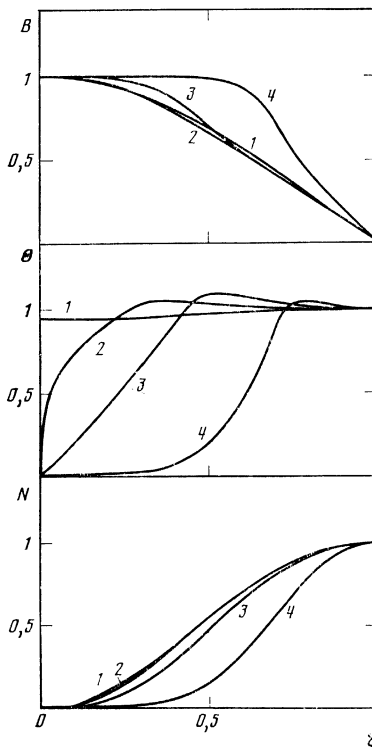


FIG. 1. Self-similar profiles of the magnetic field, temperature, and density for a magnetized plasma. Curves 2 to 4 are plotted for ζ equal to $1/4$, 2, 8, and 32, respectively.

action of heat extraction, which increases with time in accordance with (3.24), from the surface of a shell whose heat capacity is stipulated to be low.

It can be seen from Fig. 1 that near the boundary ($\xi = 1$) the temperature profile is flat, owing to the heat-conduction spreading at not too large Reynolds numbers. Taking this into account we obtain approximate analytic solutions that are quite accurate. Indeed, at $Y \equiv 1$ Eq. (4.3) becomes a Bessel function, and its solution that satisfies the boundary conditions is

$$B(\xi) = J_0(j_{0,1}\xi), \quad (4.9)$$

where $j_{0,1} = 2.405$ is the first positive root of the Bessel function $J_0(x)$. The corresponding eigenvalue is

$$\mu^2(\xi) = j_{0,1}^2 = \text{const}, \quad (4.10)$$

whence we get for the effective magnetic Reynolds number the estimate

$$\text{Rm}_{eff} \approx \text{Rm}_0 / j_{0,1}^2. \quad (4.11)$$

For low values of Rm_0 the approximate solution (4.9) and the estimate (4.11) are quite accurate; thus, at $\text{Rm}_0 \leq 100$ the error of (4.11) does not exceed 2% (see Fig. 1, and Fig. 4 below). At very large Reynolds numbers ($\text{Rm}_0 \gtrsim 1000$) the solutions of Eqs. (4.3) and (4.4), just as in Sec. 3, describe the formation of a narrow boundary layer near the wall, and the relation (4.11) between Rm_{eff} and Rm_0 assumes an asymptotic form similar to (3.40).

Comparing the foregoing with the results of the preceding section, we see that in this case the thermal conductivity and the thermopower make no diamagnetic contribution, and even decrease the compression-induced loss of the magnetic flux. The reason is that the thermal conductivity smears out the temperature profile, increasing the temperature and the conductivity of the plasma near the axis, where the Joule heat released is low. In addition, in the most important plasma region near the axis, where the major part of the current flows (except for a very narrow region near or inside the shell under real conditions), the magnetic-field and temperature gradients are oppositely directed, so that the thermoforce, as can be seen from Eq. (4.1), leads to an effective decrease of the magnetic viscosity ν_m .

5. NUMERICAL SIMULATION OF PLASMA COMPRESSION BY A SHELL

To study the dynamics of plasma compression by a shell under real conditions, when the flow as a whole is not self-similar, the system (2.1)–(2.5) was solved with a computer. We used in the numerical calculations the general (and not the asymptotic as in Secs. 3 and 4) expressions for the transport coefficient of a classical plasma.¹⁰ To clarify the influence of the shell on the compression of a magnetic field, several models of the shell were used. We considered an incompressible and nonconducting shell with specified mass per unit length along the z axis and with two limiting plasma-compression thermal regimes: 1) The heat capacity of the shell was assumed to be zero and a zero temperature gradient was postulated on its boundary (this corresponds exactly to the boundary conditions for the self-similar solutions of Sec.

3 and 4). 2) The shell heat capacity C_{sh} was assumed to be infinite, and the thermal contact of the plasma with the shell ideal, i.e., the plasma temperature at the boundary was maintained at a specified constant level during the entire compression process. The second limiting case considered for the purpose of assessing the role of the compressibility and conductivity of the shell was an idealized model of an initially cold ($T_{sh}(0) = 0.3$ eV) plasma shell with an ideal-plasma equation of state

$$P = (Z_{sh} + 1) \frac{\rho RT}{A_{sh}}, \quad \mathcal{E} = (Z_{sh} + 1) \frac{\rho RT}{(\gamma - 1) A_{sh}} \quad (5.1)$$

(R is the gas constant, A_{sh} and Z_{sh} are respectively the atomic weight of the shell material and the average ion charge in the shell) and with plasma transport coefficients.

Equations (2.1)–(2.5) were integrated with initial conditions corresponding to a plasma cylinder that is uniform and immobile at $t = 0$:

$$u = 0, \quad H = H_0, \quad T = T_0, \quad \rho = \rho_0. \quad (5.2)$$

The boundary conditions in the plasma at $r = 0$ are:

$$u = 0, \quad \partial H / \partial r = 0, \quad \partial T / \partial r = 0. \quad (5.3)$$

For a plasma shell, no additional conditions are necessary at the plasma-shell interface $r = R - (t)$. It suffices that the mass, momentum, and energy fluxes as well as the tangential components of the electric and magnetic field components be continuous. In this case the second boundary condition is imposed on the outer boundary of the shell, at $r = R + (t)$:

$$\partial T / \partial r = 0, \quad H = H_0. \quad (5.4)$$

The shell is set in motion by a pressure pulse acting on its outer surface

$$P(t) = \begin{cases} P_m \sin(\pi t / \tau), & 0 < t < \tau \\ 0, & \tau < t \end{cases}, \quad (5.5)$$

where P_m is the maximum pressure and τ is the pressure-pulse duration. For a shell accelerated by a laser beam with flux density J , the pressure was estimated from the formula^{7,11}

$$P = 11.8 \left(\frac{A_{06}}{Z_{06}} \right)^{1/2} \left(\frac{J}{10^{14} \text{ W/cm}^2} \right)^{3/2} \text{ Mbar}. \quad (5.6)$$

Equations (2.1)–(2.5) cannot be solved for the case of an incompressible shell, and it assumed that inside the shell $H(r) = H_0 = \text{const}$. In this case the boundary conditions were set only for the plasma on the inner shell boundary $r = R - (t)$, in the form

$$H = H_0, \quad (5.7)$$

$$\frac{d^2 R^-}{dt^2} = - \frac{[P(t) - P_{pl}]}{m} 2\pi R^-; \quad (5.8)$$

$$dT/dr = 0, \quad C_{sh} = 0, \quad (5.9)$$

$$T = T_{sh}(0), \quad C_{sh} = \infty,$$

where m is the mass per unit length of the shell, and P_{pl} is the plasma pressure on the boundary with the shell.

The plasma and the shell were assumed transparent to the radiation of the plasma proper. The radiative losses in

(2.5) were assumed to be of the form

$$Q_r = Q_b + Q_s; \quad (5.10)$$

the expressions used for the energy carried away by the bremsstrahlung (Q_b) and by the synchrotron radiation (Q_s) were

$$Q_b = \frac{16}{3} \left(\frac{2\pi}{3} \right)^{1/2} \frac{e^6}{m_e^4 c^3 \hbar} n^2 T^{1/2}, \quad Q_s = \frac{4e^2}{3m_e^3 c^5} n H^2 T. \quad (5.11)$$

The integration was in terms of Lagrangian coordinates, which are the most convenient for numerical solution of one-dimensional magnetohydrodynamics problems. The system (2.1)–(2.5) was approximated by a fully conservative difference scheme accurate to second order in time and space, and constituting a modification of the scheme of Ref. 13 with account taken of the thermogalvanomagnetic effects and of the thermal conductivity of the plasma. The obtained system of difference equations was solved by simple iteration. Neumann viscosity was used to smooth out the discontinuities in the scheme.

The calculation program was verified against the self-similar solutions. By way of example, the difference between the numerical and the self-similar solutions did not exceed 1% right up to a twofold radial compression of the plasma.

The results of the numerical integration are shown in Figs. 2–6. Figure 2 shows the time dependence of the variables that characterize the plasma and magnetic-field compression (the values of H , n , and T in this figure are referred to the cylinder axis $r = 0$) for a variant with a plasma shell whose initial kinetic energy per centimeter of length was $E_0 = 3.0$ kJ/cm. The shell mass in this variant was $m = 0.35$ mg/cm, the initial radius $R_0 = 0.95$ mm, and the initial density and temperature of the plasma were respectively 10^{19} cm $^{-3}$ and 20 eV. It can be seen from Fig. 2 that the magnetic pulse duration at a level on the order of 100 MOe is about 1 ns. The asymmetry of the compression and of the expansion (the rate of expansion was lower than that of the compression) was due to magnetic-flux losses that lowered the elasticity of the plasma with the magnetic field during the course of compression. The magnetic field frozen in the expanding plasma becomes lower during the expansion than the magnetic field $H_0 = 0.2$ MOe outside the shell.

The calculations have shown that the equation of state

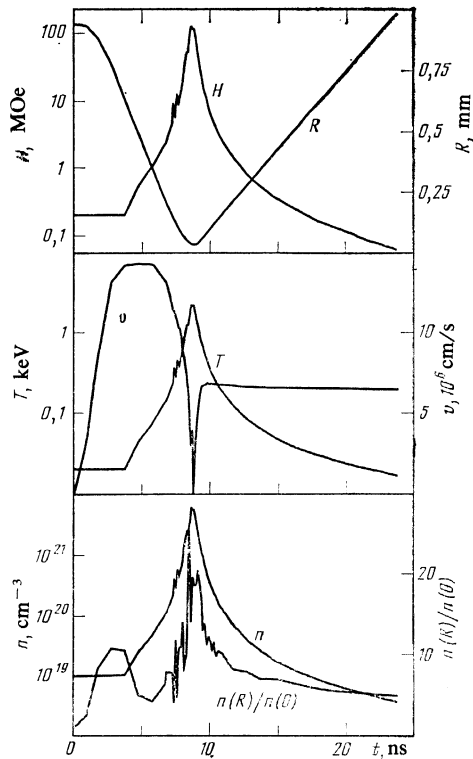


FIG. 2. Time variation of the plasma magnetic field, temperature, and density, of the plasma-boundary radius R and velocity v , and of the relative increase of the density in the boundary layer as the plasma with the magnetic field are compressed by a plasma shell with energy $E_{sh} = 1.8$ kJ/cm.

of the shell has little effect on the compression of the magnetic field. In particular, the conductivity of the shell itself influences little the confinement of the magnetic flux. Thus, for example, calculations with a plasma shell whose Coulomb conductivity was artificially lowered by two orders of magnitude, yielded a less than 10% increase of the magnetic-flux loss. The result of a substantial change of the average charge Z_{ch} of the ions in the shell is similar. The thermal regime of the shell also affects the field-compression hydrodynamics little. Calculations for both variants with incompressible shell, mentioned above, yield a compression pic-

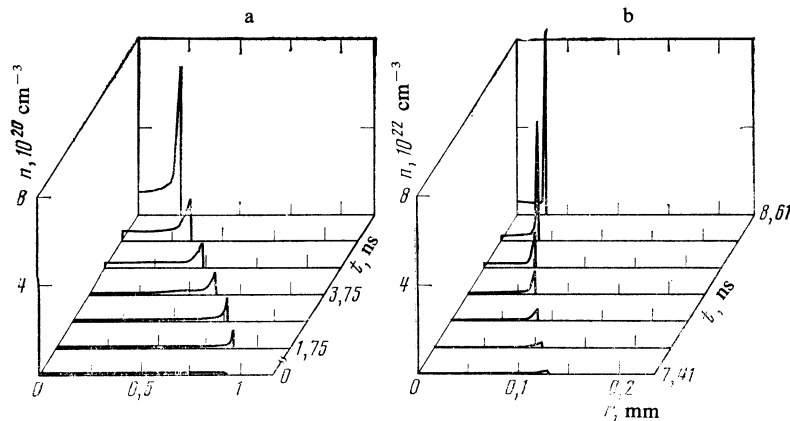


FIG. 3. Evolution of density profile in compression of a plasma by a shell under conditions of Fig. 2: a—initial compression stage, formation of boundary layer; b—near the maximum compression.

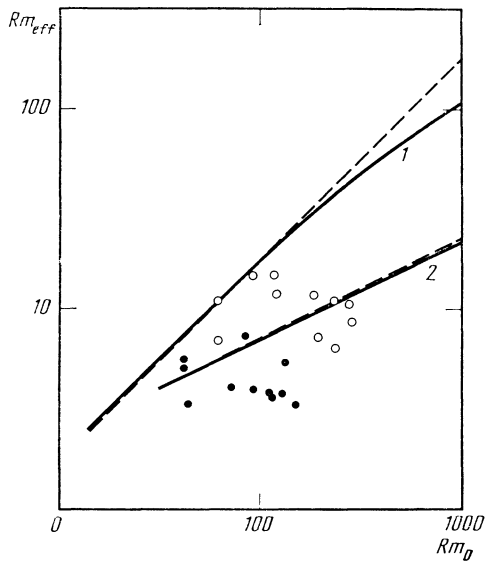


FIG. 4. Plot of Rm_{eff} vs Rm_0 for self-similar solutions corresponding to nonmagnetized and fully magnetized plasma (solid curves 1 and 2): the dashed curves represent the estimates (3.40) and (4.11). The points correspond to the results of the numerical calculations at various instants of time during the compression stage; ●—incompressible shell with zero heat capacity; ○—incompressible shell with infinite heat capacity. The remaining parameters are the same as in Fig. 3.

ture that differ from Fig. 2 by not more than several percent. Thus, the principal parameter that determines the compression of the magnetic field by the shell is the ratio δ of the initial magnetic energy inside the shell to the initial kinetic energy of the shell, thus supporting the estimates given in Refs. 1 and 4. We note that if the shell length $L \gtrsim 1$ cm, the plasma escape through the end faces of the shell can be neglected. For example, an estimate for the integral relative fraction of the mass ejected in the compression variant corresponding to Fig. 2 by the instant $t = 15$ ns of shell expansion does not exceed 10% (here $L = 1$ cm).

The most important factor for confinement of the magnetic flux and compression of the magnetic field is the formation of a narrow boundary layer in the plasma near the shell.

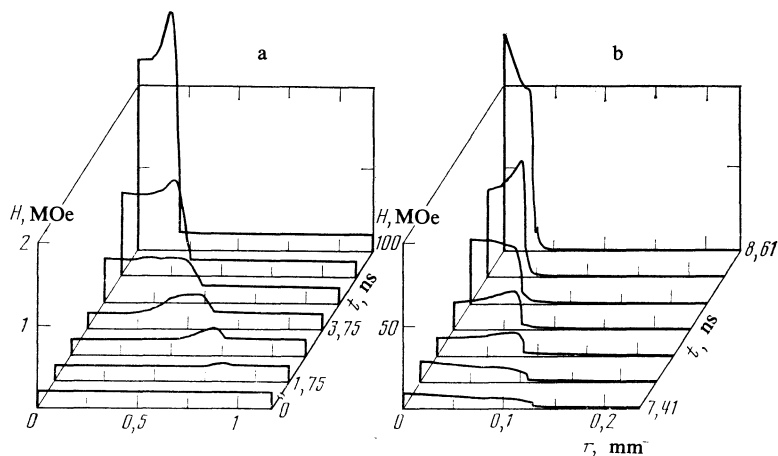


FIG. 5. Evolution of magnetic-field profile in plasma compression by a shell under the same conditions as in Fig. 3.

The plasma density in this layer is several times higher than the almost homogeneous density in the internal region (as seen from Fig. 2, the ratio $n(R)/n(0)$ during the entire compression process is in the interval 4–25). The formation of the boundary layer is illustrated in Fig. 3. It is formed already during the initial stages of the compression, and once the boundary layer in which the plasma pressure balances the magnetic pressure on the axis is formed, the flow becomes similar to that of the self-similar solutions discussed in Secs. 3 and 4 above. This is shown in Fig. 4, which shows for comparison plots of Rm_{eff} vs Rm_0 corresponding to the self-similar solutions for a nonmagnetized and fully magnetized plasma. It can be seen from Fig. 4 that the magnetic Reynolds numbers obtained by numerical calculations at various instants of plasma compression by an incompressible shell in both variants of its thermal regime agree well with the self-similar solutions. Better agreement is observed for solution 1, which corresponds to the same boundary conditions as in the self-similar solutions. In regime 2 ($C_{sh} = \infty$) the magnetic-field and temperatures in the immediate vicinity of the shell have the same direction and this, as is clear from Eq. (4.1), leads to an effective increase of the magnetic viscosity and to a corresponding decrease of Rm_{eff} .

Figure 5 shows the magnetic field profiles in the course of plasma compression by a shell. The nonuniformities of these profiles are due to the passage of sound waves through the plasma and to the associated oscillations of the magnetic field frozen into the plasma. On the whole, these profiles, just as the temperature profiles shown in Fig. 6, are qualitatively similar to the self-similar solutions considered in Secs. 3 and 4.

6. CONCLUSION

The analytic and numerical calculation show that a magnetic field frozen in a plasma can be effectively compressed by a collapsing shell. An essential fact is that, in contrast to implosive magnetic-field generators, the purpose of the shell here is to transfer its kinetic energy to the compressed plasma with the magnetic field. The contribution of the shell to the confinement of the magnetic flux is not signif-

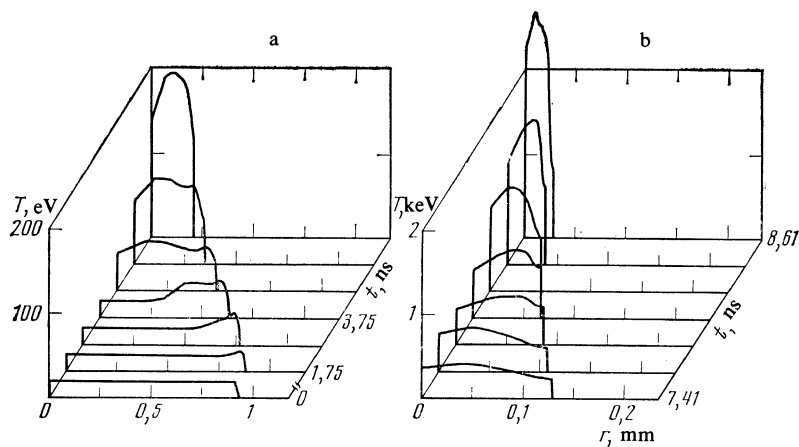


FIG. 6. Evolution of temperature profile in plasma compression by a shell under the same conditions as in Fig. 3.

icant here. Thus, many restrictions, such as the bursting of the skin layer in a metallic shell and others, applicable to impulsive magnetic-field generators, do not arise here.

It is readily seen from the parameters shown in Fig. 3 that at least the fundamental mode of the Rayleigh-Taylor instability cannot develop in the time available to stop the shell when the field is compressed.

It can be seen from the calculation results that although formation of a boundary layer near the shell does lead to an anomalously rapid loss of magnetic flux, nonetheless at reasonable values of the plasma and shell parameters the relative magnetic-field losses incurred in plasma compression are low. This confirms the energy estimates given in Refs. 1–4 and is an argument in favor of the technical feasibility of generating magnetic-field pulses of amplitude on the order of 100 MOe by the method discussed here. In particular, to obtain a magnetic-field pulse with $H_{\max} = 25$ MOe of 3 ns duration at the 20 MOe level, a shell with inside diameter 2 mm must receive an initial kinetic energy 200 J/cm at an initial field $H_0 = 0.1$ MOe inside the plasma. It can also be shown that the turbulization of a hot plasma upon compression has a negligible effect on the situation and increases the magnetic-flux loss little compared with the reported calculations with classical plasma-transport coefficients.

The authors thank A. B. Konstantinov for great help

with the numerical calculation. We are also grateful to S. I. Anisimov, Ya. B. Zel'dovich, S. P. Kapitsa, and M. I. Tribel'skiĭ for numerous helpful discussions.

¹Jaycor Co., San Diego, Cal., USA.

²The authors thank G. A. Askar'yan for calling their attention to Refs. 5 and 6.

³M. A. Liberman and A. L. Velikovich, *J. Plasma Phys.* **31**, 381 (1984).

⁴G. D. Bogomolov, A. L. Velikovich, and M. A. Liberman, *Pis'ma Zh. Tekh. Fiz.* **9**, 748 (1983) [*Sov. J. Tech. Phys. Lett.* **9**, 322 (1983)].

⁵F. S. Felber, Western Research Corp. Report WRC-676-V, September 1983.

⁶F. S. Felber, M. A. Liberman, and A. L. Velikovich, *Appl. Phys. Lett.* (1985) (to be published).

⁷G. A. Askar'yan, V. A. Namiot, and M. S. Rabinovich, *Pis'ma Zh. Eksp. Teor. Fiz.* **17**, 597 (1973) [*JETP Lett.* **17**, 424 (1973)].

⁸G. A. Askar'yan, *ibid.* **28**, 322 (1977) [**28**, 296 (1977)].

⁹G. H. McCall, *Plasma Phys.* **25**, 237 (1983).

¹⁰H. Knoepfel, *Pulsed High-Energy Fields*, North Holland, 1970.

¹¹G. E. Vekshteĭn, *Dokl Akad. Nauk SSSR* **271**, 98 (1983) [*Sov. Phys. Doklady* **28**, 569 (1983)].

¹²S. I. Braginskii, *Voprosy teorii plazmy (Problems of Plasma Theory)*, Vol. 1, Atomizdat, 1963, p. 183.

¹³D. Saltzman, S. Eliezer, A. D. Mrumbein, and L. Gitter, *Phys. Rev.* **A28**, 1738 (1983).

¹⁴A. A. Samarskiĭ and Yu. P. Popov, *Raznostnye skhemy gazovoi dinamiki (Difference Schemes in Gasdynamics)*, Nauka, 1975.

Translated by J. G. Adashko